



ClampFISH detects individual nucleic-acid molecules using click chemistry based amplification

Sara H. Rouhanifard¹, Ian A. Mellis^{1,2}, Margaret Dunagin¹, Sareh Bayatpour¹, Connie L. Jiang^{1,3}, Ian Dardani¹, Orsolya Symmons¹, Benjamin Emert^{1,2}, Eduardo Torre^{1,4}, Allison Cote¹, Alessandra Sullivan⁵, John A. Stamatoyannopoulos⁵, and Arjun Raj^{1,2,6}

¹Department of Bioengineering, University of Pennsylvania, Philadelphia PA

²Genomics and Computational Biology Group, Perelman School of Medicine, University of Pennsylvania, Philadelphia PA

³Cell and Molecular Biology Group, Perelman School of Medicine, University of Pennsylvania, Philadelphia, PA

⁴Department of Biochemistry and Biophysics, Perelman School of Medicine, University of Pennsylvania, Philadelphia PA

⁵Altius Institute for Biomedical Sciences, Seattle, WA

⁶Department of Genetics, Perelman School of Medicine, University of Pennsylvania, Philadelphia PA

Abstract

Methods for detecting single nucleic acids in cell and tissues, such as fluorescence in situ hybridization (FISH), are limited by relatively low signal intensity and non-specific probe binding. Here we present click-amplifying FISH (clampFISH), a method for fluorescence detection of nucleic acids that achieves high specificity and high-gain (>400x) signal amplification. ClampFISH probes form a “C” configuration upon hybridization to the sequence of interest in a double helical manner. The ends of the probes are ligated together using bioorthogonal click chemistry, effectively locking the probes around the target. Iterative rounds of hybridization and click amplify the fluorescence intensity. We show that clampFISH enables the detection of RNA species with low magnification microscopy and in RNA-based flow cytometry. Additionally, we show that the modular design of clampFISH probes allows multiplexing of RNA and DNA detection, that the locking mechanism prevents probe detachment in expansion microscopy, and that clampFISH can be applied in tissue samples.

Single molecule RNA fluorescence *in situ* hybridization (RNA FISH), which enables the direct detection of individual RNA molecules^{1,2,3}, has emerged as a powerful technique for

Users may view, print, copy, and download text and data-mine the content in such documents, for the purposes of academic research, subject always to the full Conditions of use:http://www.nature.com/authors/editorial_policies/license.html#terms

Contributions: S.H.R. and A.R. designed the study and wrote the manuscript. I.A.M. performed statistical analysis. S.H.R., M.D., S.B., C.L.J., I.D., O.S., B.E., E.T., A.C., A.S. and J.A.S. designed and performed the experiments.

Competing interests:

A.R. receives royalties related to Stellaris RNA FISH probes.

measuring both RNA abundance and localization in single cells. Yet, while single molecule RNA FISH is simple and robust, the total signal generated by single molecule RNA FISH probes is low, thus requiring high-powered microscopy for detection. This keeps throughput relatively low and precludes the use of downstream detection methods such as flow cytometry. As such, amplification methods for single molecule RNA FISH with high efficiency, specificity and gain could enable many new applications.

A number of signal amplification techniques are available, but each suffers from particular limitations due to dependence on enzymatic activity or hybridization alone for signal gain. Approaches such as tyramide signal amplification (TSA)⁴, or enzyme ligated fluorescence (ELF)⁵ utilize enzymes to catalyze the deposition of fluorescent substrates near the probes. Alternatively, in techniques such as rolling-circle amplification (RCA), enzymes ligate oligonucleotides to form a circular probe and then catalyze a “rolling circle” nucleic acid amplification to generate a repeating sequence, which can be detected using fluorescent oligonucleotides^{6–8}. These methods can lead to large signal gains, but are limited by the accessibility of (sometimes multiple) bulky enzymes that need to diffuse through the fixed cellular environment to reach their target molecules. For example, the DNA ligases frequently used to circularize padlock probes are often quite inefficient⁹, contributing to inconsistent amplification¹⁰.

Non-enzymatic amplification schemes, most notably the hybridization chain reaction (HCR)^{11–13} and branched DNA (bDNA)^{14–16} techniques rely only on hybridization to amplify signal. Their larger DNA scaffolds, to which fluorescent probes attach, often have limited amplification potential¹⁷ and generally lack assay design flexibility for multiplexing. Thus, our goal was to create a non-enzymatic, exponential amplification scheme with high sensitivity (detection efficiency), very high gain (signal amplification), and specificity (low background).

We first designed probes that would bind with high specificity and sensitivity; i.e., that could allow the probes to survive repeated liquid handling in conditions stringent enough to limit nonspecific binding and thus prevent spurious amplification. Padlock probes are a class of circular DNA probes that have these properties: they bind to the target region of complementarity via the 5' and 3' ends of the probe, with the intervening sequence not hybridized to the target in a “C” configuration.¹⁸ Conventionally, the ends are then connected using a DNA or RNA¹⁹ ligase. This connection, in combination with the DNA:RNA double helix formed upon hybridization, result in a molecule that is physically wrapped around the target strand (Figure 1a). We wished to retain the benefits of padlock probes without the need for this enzymatic ligation; therefore, we designed padlock-style probes with terminal alkyne and azide moieties at the 5' and 3' ends (click-amplifying FISH (clampFISH) probes; Figure 1a, Supplementary Figure 1). When the clampFISH probe hybridizes to the target RNA, the DNA:RNA hybrid brings the two moieties together in physical space. We then used a click chemistry strategy (copper(I)-catalyzed azide-alkyne cycloaddition, CuAAC²⁰) to covalently link the 5'-alkyne and 3'-azide ends of the probe, effectively forming a loop around the target RNA (Figure 1a).

To achieve exponential amplification, we first designed a series of primary clampFISH probes to target the RNA sequence of interest. The backbone of each primary clampFISH probe contains two “landing pads” for a set of secondary, fluorescent, clampFISH probes. The number of landing pads may be modified to increase amplification (Supplementary Figure 1). To the backbones of these secondary probes, we hybridized a set of tertiary probes that bound in a 2:1 ratio. In a subsequent round, the secondary probes again bind 2:1 to the backbones of tertiary probes and so on, thereby in principle doubling the signal in each round (Figure 1b). The resulting probes bind efficiently to the target, as evidenced by the colocalization of clampFISH probes with single molecule RNA FISH probes targeting the same RNA (Figure 1c, Supplementary Figure 2). We have observed that many non-colocalizing spots often correspond to faint smFISH spots that are not picked up by our thresholding software for smFISH. The absence of clampFISH spots in our genetic negative controls suggests that these faint spots may in fact be true positive signal. The number of amplification rounds may be adjusted based on the desired degree of amplification required for the particular application (Figure 1d).

To demonstrate exponential amplification using clampFISH probes, we first targeted and amplified GFP mRNA in a human melanoma cell line (WM983b) stably expressing GFP²¹ using a set of 10 primary clampFISH probes (Figure 1e). We used stringent hybridization conditions—specifically, a higher concentration of formamide than is traditionally used for single molecule RNA FISH—to limit nonspecific probe binding while still allowing for specific binding (Supplementary Figure 3). As the number of rounds progressed, the average number of spots per cell remained constant (for example, at round 2 we detected a mean of 399 spots per cell \pm 62 and at round 10 we detected 401 spots per cell \pm 36; Figure 1f), while the intensity of the signal as measured by fluorescence microscopy increased. At round 12, the mean signal per spot was 446-fold higher than in round 2 (Figure 1i). We observed a 3.39-fold \pm 1.29 increase (geometric mean and geometric standard deviation of fold changes in average spot intensity in 2-round intervals from round 2 – 12) for every two rounds of amplification (for an average 1.69-fold increase per round; Figure 1g-i). We also observed that the fold-amplification decreases slightly at later rounds, and we estimate that the saturation point, i.e., the estimated point at which no further amplification would occur, would be reached around round 20 (Supplementary Figure 4).

To assess whether the click reaction aided in the amplification process as hypothesized, we performed the same experiment in the absence of the click-ligation of the clampFISH probes. Although the number of spots detected per cell were similar (393 mean spots per cell in the clicked samples vs. 381 mean spots per cell in the non-clicked samples), we observed lower mean signal intensity (26,076 AU \pm 496 for non-clicked vs. 44,450 AU \pm 630 for clicked samples at round 12) as well as a lack of uniformity in spot intensity (coefficient of variation at round 12 for non-clicked cells = 0.94 \pm 0.013 vs. 0.69 \pm 0.01 for clicked cells), demonstrating that the click reaction facilitated a more uniform and higher gain amplification of clampFISH signal (Figure 1h, Supplementary Figure 5). (Figure 1h).

To demonstrate signal specificity, we performed the same clampFISH detection and amplification on the parental cell line that did not have the GFP gene. We detected very few false-positive spots in these cells (mean of 9.77 spots per cell \pm 1.45), showing that the

signals were specific to the target (Figure 1e). Although this number is low, it may interfere with the detection of RNAs with few transcripts per cell.

Owing to its relatively low signal intensity, single molecule RNA FISH typically requires using a microscope equipped with a high numerical aperture oil immersion objective. For many applications, a low magnification air objective is preferable, both for increased throughput and for simplicity of sample handling. We reasoned that the increased signals that clampFISH provided could make RNA FISH signals detectable by low magnification microscopy (Figure 2a). To test this, we mixed 20% WM983b cells stably expressing GFP with 80% WM983b cells without GFP and probed for GFP mRNA using clampFISH probes at round 6—this was the minimum number of rounds needed to clearly discern signal at the lowest magnification for this particular target. Using clampFISH, the positive cells were clearly discernible at both 20X and 10X magnification, whereas the conventional single molecule RNA FISH signal was not (Figure 2a). To demonstrate the speed of image acquisition for high throughput applications, we applied clampFISH to detect *HIST1H4E*, an RNA target lacking a corresponding antibody for detection (Figure 2b, Supplementary Figure 6). Scanning one well of a 96 well plate took ~21 minutes at 20x magnification using clampFISH as opposed to ~4 hours at 60x magnification using single molecule RNA FISH.

Primary tissue samples typically suffer from high background levels that contribute to a low signal-to-noise ratio using single molecule RNA FISH, and therefore require high magnification microscopy to discern positive signal from background. However, at high magnification, large structural features of the tissue are often difficult to discern, and tiled image scanning is relatively slow. To increase the field of view while still imaging individual RNAs, we applied 4-rounds of clampFISH to 4 day old C57BL/6J mouse kidney samples and probed for *Podxl* mRNA, a gene that is highly expressed in podocytes²², and observed specific clampFISH signal in the appropriate regions (Figure 2c, Supplementary Figure 7). ClampFISH further revealed that *Podxl* is also expressed in the kidney endothelium, a signal that was only faintly visible by single molecule RNA FISH, but was clearly detected by clampFISH at low magnification (Figure 2c). This is consistent with previous findings that *Podxl* is expressed at low levels in the kidney endothelium²³ and highlights the utility of clampFISH for detection of low abundance transcripts in tissue.

Another application that clampFISH enables is flow cytometry-based measurement of RNA expression, an application for which single molecule RNA FISH typically does not produce enough signal^{24,25}. We applied clampFISH to a mixed population of MDA-MB 231 cells with and without GFP expression and analyzed the cells by flow cytometry (Figure 2d, Supplementary Figure 8,9), using GFP fluorescence as an independent measure of the specificity of clampFISH signal. We observed separation of GFP positive cells by clampFISH signal with as few as 2 rounds of amplification, and observed a 2.447-fold increase in fluorescence intensity in the GFP positive population with every 2 rounds of amplification thereafter (geometric mean of fold change across rounds; Figure 2d, Supplementary Figure 8). Notably, we observed a decreasing fold-change as we moved through the rounds (3.435-fold from rounds 2–4, 2.589-fold from rounds 4–6, and 1.648-fold from rounds 6–8). We also used clampFISH to sort cells based on endogenous RNA

expression for *HIST1H4E* mRNA and the lncRNA *NEAT1* (Figure 2e), relatively low abundance targets that cannot be detected using antibodies.

Amplification of RNA signal can also be used in combination with a newly developed expansion microscopy technique that achieves super-resolution microscopy via the physical expansion of cells embedded in polymeric hydrogels^{26,27}. When combined with single molecule RNA FISH, expansion microscopy can resolve the fine structure of RNAs that are in close proximity to one another; however, the physical expansion of cells results in reduced signal intensities, at least partially due to probes dissociating under the low salt conditions required to obtain high levels of hydrogel expansion. We reasoned that the locking property of clampFISH probes would allow us to maintain signal intensity in the face of these expansion conditions. We thus performed clampFISH on GFP mRNA to round 6 followed by expansion and observed high signal intensity on all spots when the click reaction was performed, but with little signal when click was not performed (Figure 2d, Supplementary Figure 10). We also applied clampFISH to amplify *NEAT1* to round 6, a nuclearly retained long non-coding RNA, and observed higher signal intensity than with single molecule RNA FISH (Figure 2d, Supplementary Figure 10). This also suggests that clampFISH probes are accessible to the nucleus, which can be a problem with other amplification schemes¹⁶. Notably, we also observed nuclear localization of the GFP mRNA using clampFISH probes (Figure 1c and e), but did not detect transcription sites. Upon further analysis, we determined that clampFISH probes can enter the nucleus but may have difficulty accessing transcription sites (data not shown), possibly due to crowding from RNA secondary structure or nearby proteins.

A key design goal for FISH methods is the ability to detect multiple RNA targets simultaneously. Multiplexing with clampFISH is in principle straightforward because of the modular design of the probes. The backbone sequence of the clampFISH probes can easily be changed, allowing one to use multiple independent amplifiers simultaneously. Many transcripts may be amplified simultaneously with unique backbone sequences that are not labeled with a fluorophore, and the subsequent loop-dendrimer structure can be probed with fluorescently labeled secondary fluorescent oligonucleotides that can be easily removed and re-hybridized. As a proof-of-concept, we selected 3 RNA targets with distinct expression patterns in HeLa cells: *NEAT1*, which is found in nuclear paraspeckles of most cells; *LMNA*, which is found in the cytoplasm of all cells, and *HIST1H4E*, which expresses only in the subpopulation of cells that are in S phase. We amplified these with unique sets of non-fluorescent clampFISH probes to 7 rounds, then probed the terminal backbones with single molecule RNA FISH probes, each labeled with different fluorophores (Figure 3a, Supplementary Figure 11). We were able to visualize signals from the three different probe sets, even using low magnification microscopy. We observed that *LMNA* was present in nuclear paraspeckles and therefore colocalized with the *NEAT1* signal. We confirmed that this was not bleedthrough by imaging each probe, amplified to 7 rounds in every channel using the same exposure times and observing no signal in the off-channels (Supplementary Figure 11).

Our method for the amplification of fluorescent RNA signals *in situ* is different from other non-enzymatic, hybridization-based technologies because it directly links the probe to the

target RNA whereas other systems are susceptible to probe detachment during washes. In a direct comparison with commercially available systems, we observed that other methods' maximum fluorescence intensity amplification is comparable to clampFISH at 6 rounds (Supplementary Figure 12), however, the fluorescence intensity of clampFISH far surpasses other methods beyond round 6. Thus, the clampFISH amplification system can enable assays that require extremely high signal gain, especially flow cytometry (Figure 2c) and high throughput microscopy of targets with lower expression levels (Figure 3a). For instance, we were able to detect *HIST1H4E* RNA with low-power microscopy even though it is typically expressed at levels of only around 200 molecules per cell²¹ (Figure 3a).

Additional benefits of clampFISH include tunable, exponential amplification of fluorescence intensity (Figure 1), modular probe design for simplified and expanded multiplexing capabilities, and compatibility with expansion microscopy. Notably, the ends of the clampFISH probes behave as a proximity ligation wherein the click reaction will occur if and only if the two arms are hybridized adjacent to each other (Supplementary Figure 13), suggesting that clampFISH may find uses in specifically probing RNA subsets such as splicing junctions, short alternatively spliced variants, or edited RNAs. Finally, we applied a modified clampFISH hybridization scheme to detect 5S rDNA²⁸ loci in single cells (Figure 3b, Supplementary Figure 14). The stringent hybridization conditions of DNA FISH are not typically compatible with RNA FISH. When we performed *HIST1H4E* RNA clampFISH prior to 5S rDNA clampFISH, we found that the probes can survive these steps and enable simultaneous amplification and imaging of both DNA and RNA (Figure 3c, Supplementary Figure 14)

Online Methods

Cell culture.

We cultured WM983b cells and WM983b-GFP-NLS cells (a human metastatic melanoma cell line from the lab of Meenhard Herlyn) in tumor specialized media containing 2% FBS. The WM983b-GFP-NLS contains EGFP fused to a nuclear localization signal driven by a cytomegalovirus promoter that we stably transfected into the parental cell line.

Clamp probe design and synthesis.

Clamp probes are 150 nt long (15mer left RNA binding arm, 10 nt left adapter, 100mer backbone, 10 nt right adapter, 15mer right RNA binding arm). RNAs are targeted by probe sets containing one or more Clamp probes, each targeting a 30 nt region of RNA (2 adjacent 15mer binding arms). We chose binding regions with approximately 40% GC content as well as minimal repetitive regions using our probe design pipeline (source code available here: <https://flintbox.com/public/project/50547/>) and instructions for use are available in the **supplementary methods**. We designed backbones so as to minimize predicted secondary structure (using mFold; <http://unafold.rna.albany.edu/?q=mfold>). We ordered modified DNA oligonucleotides from Integrated DNA Technologies (IDT) as standard DNA oligonucleotides with modifications (5'-phosphate on the backbone, 3'-azide and 5'-phosphate for the right arm and 5'-hexynyl for the left arm). Strands were resuspended in nuclease free water, at a working stock concentration of 400 μ M. The left arm (30 μ M),

backbone (20 μM) and right arm (30 μM) are brought together using adapter probes (30 μM each) and denatured at 70°C for 3 min prior to being enzymatically ligated using 600 U of T7 DNA ligase (New England Biolabs) for a minimum of 1 hour at room temperature. Following ligation, the probes were purified using Monarch purification columns according to manufacturer's instructions (New England Biolabs) and eluted in 4X the starting volume to make the working dilution. For a schematic protocol and probe sequences, see Supplementary figure 1 and Supplementary table.

ClampFISH procedure on cultured cells.

We grew cells on glass coverslides until ~70% confluent. We washed the cells twice with 1X PBS, then fixed for 10 minutes with 4% formaldehyde/1X PBS at room temperature. We aspirated off the formaldehyde, and rinsed twice with 1X PBS prior to adding 70% ethanol for storage at 4°C. We incubated our cells for at least 4 hours at 37°C in hybridization buffer (10% dextran sulfate, 2X SSC, 20% formamide) and 0.5 μl of the working dilution of the primary ClampFISH probe. We performed two washes in wash buffer (2X SSC, 10% formamide), each consisting of a 30-min incubation at 37°C. We then incubated the cells for at least 2 hours at 37°C in hybridization buffer (10% dextran sulfate, 2X SSC, 20% formamide) and 1 μl of the working dilution of the secondary ClampFISH probe and repeated the washes. After the second wash, we performed the 'click' reaction. A solution containing 75 μM $\text{CuSO}_4 \cdot 5\text{H}_2\text{O}$ premixed with 150 μM BTAA ligand²⁰ (Jena Biosciences) and 2.5 mM sodium ascorbate (made fresh and added to solution immediately before use; Sigma) in 2X SSC was added to the samples, and these were then incubated for 30 min at 37°C. The samples were then rinsed briefly with wash buffer, then we continued cycling this protocol, alternating between secondary and tertiary ClampFISH probes until reaching the desired level of amplification. After the final wash, we rinsed once with 2X SSC/DAPI and once with anti-fade buffer (10 mM Tris (pH 8.0), 2X SSC, 1% w/v glucose). Finally, we mounted the sample for imaging in an anti-fade buffer with catalase (Sigma) and glucose oxidase² (Sigma) to prevent photobleaching. This method is described in more detail in the Supplementary working protocol.

ClampFISH for flow cytometry and sorting.

ClampFISH for flow cytometry was performed as described above however the cells were kept in suspension. Wash buffer and 2X SSC were supplemented with 0.25% Triton-X, and the clampFISH hybridization buffer was supplemented with the following blocking reagents: 1 $\mu\text{g}/\mu\text{l}$ yeast tRNA (Invitrogen), 0.02% w/v bovine serum albumin, 100ng/ μl sonicated salmon sperm DNA (Agilent). We sorted on NEAT1 and HIST1H4E RNA abundance using a FACSJazz (BD Biosciences) with 640nm excitation laser and 660/20 nm emission detector.

ClampFISH for expansion microscopy.

Acryloyl-X, SE (6-((acryloyl)amino)hexanoic acid, succinimidyl ester, here abbreviated AcX; Thermo-Fisher) was resuspended in anhydrous DMSO at a concentration of 10 mg/mL, aliquoted and stored frozen in a desiccated environment. Label-IT[®] Amine Modifying Reagent (Mirus Bio, LLC) was resuspended in the provided Mirus Reconstitution Solution at 1mg/ml and stored frozen in a desiccated environment. To prepare LabelX, 10

μL of AcX (10 mg/mL) was reacted with 100 μL of Label-IT® Amine Modifying Reagent (1 mg/mL) overnight at room temperature with shaking. LabelX was subsequently stored frozen ($-20\text{ }^{\circ}\text{C}$) in a desiccated environment until use.

Fixed cells were washed twice with $1\times$ PBS and incubated with LabelX diluted to 0.002 mg/mL in MOPS buffer (20 mM MOPS pH 7.7) at $37\text{ }^{\circ}\text{C}$ for 6 hours followed by two washes with $1\times$ PBS. Monomer solution ($1\times$ PBS, 2 M NaCl, 8.625% (w/w) sodium acrylate, 2.5% (w/w) acrylamide, 0.15% (w/w) N,N'-methylenebisacrylamide) was mixed, frozen in aliquots, and thawed before use. Prior to embedding, monomer solution was cooled to $4\text{ }^{\circ}\text{C}$ to prevent premature gelation. Concentrated stocks (10% w/w) of ammonium persulfate (APS) initiator and tetramethylethylenediamine (TEMED) accelerator were added to the monomer solution up to 0.2% (w/w) each. 100 μL of gel solution specimens were added to each well of a Lab Tek 8 chambered coverslip and transferred to a humidified $37\text{ }^{\circ}\text{C}$ incubator for two hours.

Proteinase K (New England Biolabs) was diluted 1:100 to 8 units/mL in digestion buffer (50 mM Tris (pH :8, 1 mM EDTA, 0.5% Triton X-100, 0.8 M guanidine HCl) and applied directly to gels in at least ten times volume excess. The gels were then incubated in digestion buffer for at least 12 hours. Gels were then incubated with wash buffer (10% formamide, $2\times$ SSC) for 2 hours at room temperature and hybridized with RNA FISH probes in hybridization buffer (10% formamide, 10% dextran sulfate, $2\times$ SSC) overnight at $37\text{ }^{\circ}\text{C}$. Following hybridization, samples were washed twice with wash buffer, 30 minutes per wash, and washed 4 times with water, 1 hr per wash, for expansion. Samples were imaged in water with $0.1\mu\text{g/mL}$ DAPI.

ClampFISH for mouse tissues.

All studies were carried out under a protocol approved by the Institutional Animal Care And Use Committee at the University of Pennsylvania. Kidneys were harvested from 4 day old C57BL/6J mice. Dissected tissues were embedded in OCT, then flash frozen using liquid nitrogen. $5\text{ }\mu\text{m}$ tissue sections were cut at $-20\text{ }^{\circ}\text{C}$ and mounted on charged slides. Slides were washed briefly in PBS, then immersed in 4% paraformaldehyde for 10 min at room temperature. Following fixation, the slides were transferred to 70% ethanol for permeabilization for at least 12 hours, or for long-term storage. To begin clampFISH procedure, slides were transferred to wash buffer for 3 minutes to equilibrate, then 500 μL of 8% SDS was added to the top of the flat slide for 1 minutes for tissue clearing. Samples were transferred to wash buffer, and normal clampFISH procedure was used.

ClampFISH for multiplexing.

Primary clampFISH probes for multiple targets (each with a different backbone series) are hybridized and washed at the same time. Each subsequent round is performed together using the respective secondary and tertiary probes that are colorless. After the terminal round, samples are washed with 10% formamide/ $2\times$ SSC, then hybridized with RNA FISH probes in hybridization buffer (10% formamide, 10% dextran sulfate, $2\times$ SSC) overnight at $37\text{ }^{\circ}\text{C}$. Following hybridization, samples were washed twice with wash buffer, 20 minutes per wash, then counterstained with DAPI nuclear stain and prepared for imaging.

DNA clampFISH on cultured cells.

Probe design is performed the same as with RNA targets, however with 30mer left and right arms. We grew cells on glass coverslips until ~70% confluent. We washed the cells twice with 1X PBS, then fixed for 10 minutes with 4% formaldehyde/1X PBS at room temperature. We aspirated off the formaldehyde, and rinsed twice with 1X PBS prior to adding 70% ethanol for storage at 4°C. We washed the cells 2X for 5 min in 1X PBS, then permeabilized the cells for 15 min at room temperature with 1X PBS supplemented with 0.5% Triton X-100. We washed the cells 2X with 1X PBS, then treated the cells with 0.1M HCl for 5 min. We washed the cells 2X with 2X SSC, then treated with an optional incubation of 25 µg/ml RNase A for 30 min at 37°C. Cells were washed 2X with 2X SSC, then equilibrated with 50% formamide in 2X SSC for 30 min. Liquid was aspirated and cells were denatured using 70% formamide/2X SSC on a hot plate at 78°C for 4.5 min. We incubated our cells for at least 4 hours at 37°C in hybridization buffer (10% dextran sulfate, 2X SSC, 50% formamide) and 0.5 µl of the working dilution of the primary DNA clampFISH probe. Washes and subsequent rounds of clampFISH were done using the standard clampFISH procedure.

Comparison of amplification methods.

GFP mRNA clampFISH was performed to round 6 according to the protocol reported above on WM983b-GFP and WM983b cells. These probes were Cy5 labeled, and signal intensity was compared to a corresponding smFISH probe set targeting GFP mRNA that was also labeled with Cy5. GFP mRNA was also detected using RNAscope technology according to the manufacturer's protocol (ACDbio). These probes were ATTO 647 labeled, and signal intensity was compared to a corresponding smFISH probe set targeting GFP mRNA that was also labeled with ATTO 647. GFP mRNA was also detected using HCR technology according to the manufacturer's protocol (Molecular Instruments). These probes were Alexa 647 labeled, and signal intensity was compared to a corresponding smFISH probe set targeting GFP mRNA that was also labeled with Alexa 647.

Imaging.

We imaged each samples on a Nikon Ti-E inverted fluorescence microscope a cooled CCD camera (Andor iKon 934). For 100× imaging, we acquired z-stacks (0.3 µm spacing between stacks) of stained cells. The filter sets we used were 31000v2 (Chroma), 41028 (Chroma), SP102v1 (Chroma), 17 SP104v2 (Chroma) and SP105 (Chroma) for DAPI, Atto 488, Cy3, Atto 647N/Cy5 and Atto 700, respectively. A custom filter set was used for Alexa 594 (Omega). We varied exposure times depending on the dyes and degree of amplification used. Typically, ClampFISH imaging was done at a 300 ms exposure and single molecule RNA FISH was done at 2–3 s exposure.

Image analysis.

We first segmented and thresholded images using a custom MATLAB software suite (downloadable at <https://bitbucket.org/arjunrajlaboratory/rajlabimagetools/wiki/Home>). Segmentation of cells was done manually by drawing a boundary around non-overlapping cells. Unless otherwise specified, we called clampFISH and single molecule RNA FISH

spots using the previously described algorithm in rajlabimagetools (<https://bitbucket.org/arjunrajlaboratory/rajlabimagetools/wiki/Home>). *For colocalization analysis: We performed spot colocalization analysis as previously described*²⁹. Briefly, after initial spot calling, the algorithm used Gaussian fitting to refine spot localization estimates, and then a 2-stage algorithm incorporating chromatic aberration correction to identify pairs of spots colocalizing across two channels. *For expansion-FISH: We manually segmented cells as described above. We performed spot calling using the modified expansion spot-calling processor in rajlabimagetools, as previously described.*

Statistical analysis.

All experiments were performed in multiple, independent experiments, as indicated in the figure legends. All statistics and tests are described fully in the text or figure legend. Error bars throughout represent standard error of the mean unless otherwise specified.

Reproducible analyses.

Scripts for all analyses presented in this paper, including all data extraction, processing, and graphing steps are freely accessible at the following url:https://www.dropbox.com/sh/b2mv4o9wmzcicqv/AABARZsKtD1TQKMseoG_LnyWa?dl=0. Our image analysis software is available here: <https://bitbucket.org/arjunrajlaboratory/rajlabimagetools/wiki/Home>, changeset 6aa67c3b68c8dd5599fed681e1a21ec674464c65. All raw and processed data used to generate figures and representative images presented in this paper are available at the following url: https://www.dropbox.com/sh/b2mv4o9wmzcicqv/AABARZsKtD1TQKMseoG_LnyWa?dl=0.

Life Sciences Reporting Summary.

Further information on experimental design and reagents is available in the Nature Research Reporting Summary linked to this article.

Supplementary Material

Refer to Web version on PubMed Central for supplementary material.

Acknowledgements:

We thank F. Tuluc from the CHOP flow cytometry core facility for helpful discussions and assistance with flow cytometry. S.H.R. acknowledges support from NIH 1F32GM120929-01A1; I.A.M. acknowledges support from NIH F30 NS100595; O.S. acknowledges support from the Human Frontier Science Program LT000919/2016-L; C.L.J. acknowledges support from NIH 5T32DK007780-19; and A.R. from NIH 4DN U01 HL129998, NIH Center for Photogenomics RM1 HG007743, the Chan Zuckerberg Initiative and HCA Pilot Project 174285, NSF CAREER 1350601, NIH R33 EB019767. We also thank Jonathan Peterson for his early contributions and the many BioRxiv readers that reached out with helpful feedback and suggestions.

References

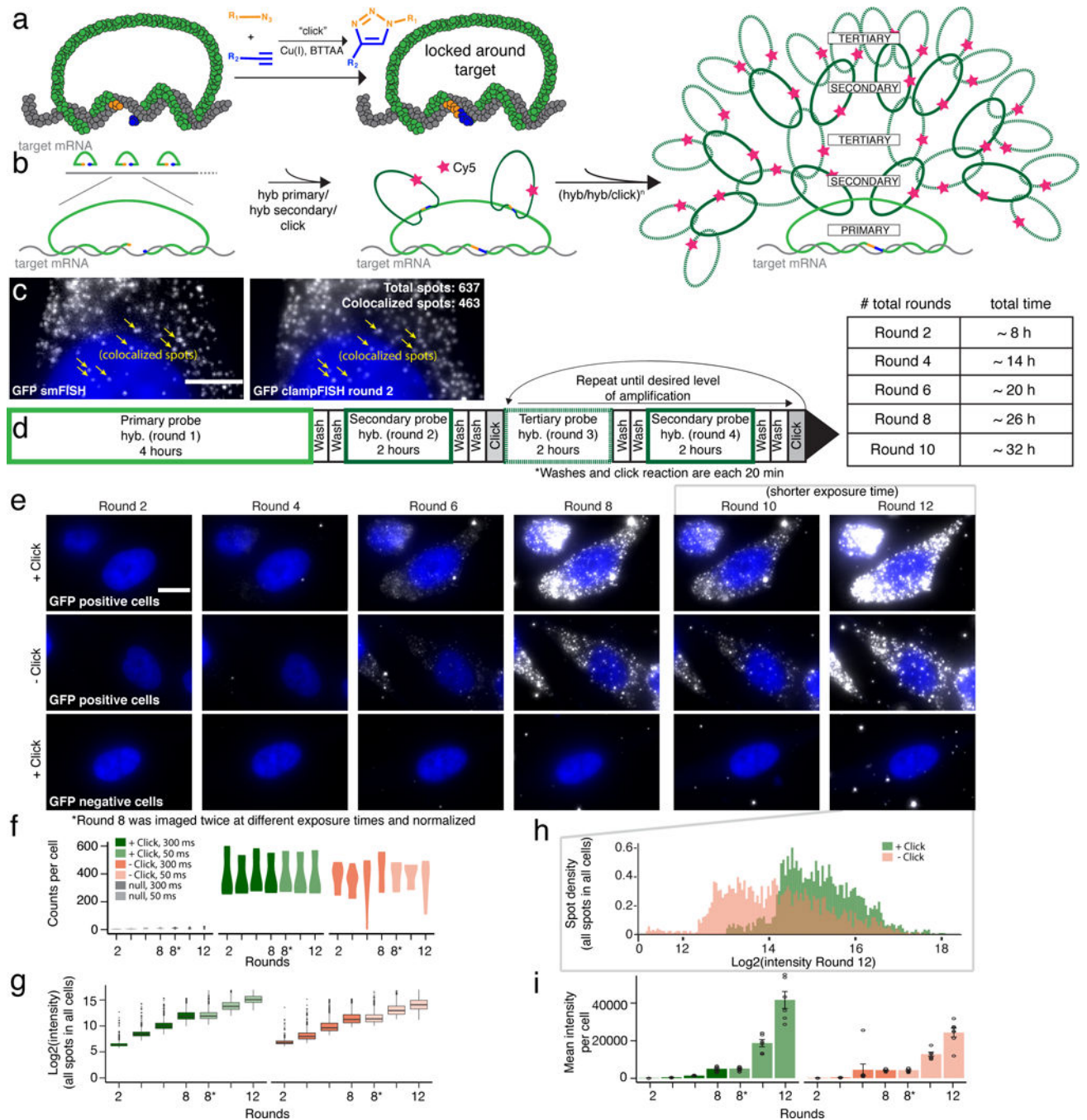
1. Femino AM, Fay FS, Fogarty K & Singer RH Visualization of single RNA transcripts in situ. *Science* 280, 585–590 (1998). [PubMed: 9554849]
2. Raj A, van den Bogaard P, Rifkin SA, van Oudenaarden A & Tyagi S Imaging individual mRNA molecules using multiple singly labeled probes. *Nat. Methods* 5, 877–879 (2008). [PubMed: 18806792]

3. Itzkovitz S & van Oudenaarden A Validating transcripts with probes and imaging technology. *Nat. Methods* 8, S12–9 (2011). [PubMed: 21451512]
4. Chen CH et al. Specific sorting of single bacterial cells with microfabricated fluorescence-activated cell sorting and tyramide signal amplification fluorescence in situ hybridization. *Anal. Chem.* 83, 7269–7275 (2011). [PubMed: 21809842]
5. Lu J & Tsourkas A Imaging individual microRNAs in single mammalian cells in situ. *Nucleic Acids Res.* 37, e100 (2009). [PubMed: 19515934]
6. Banér J, Nilsson M, Mendel-Hartvig M & Landegren U Signal amplification of padlock probes by rolling circle replication. *Nucleic Acids Res.* 26, 5073–5078 (1998). [PubMed: 9801302]
7. Larsson C, Grundberg I, Söderberg O & Nilsson M In situ detection and genotyping of individual mRNA molecules. *Nat. Methods* 7, 395–397 (2010). [PubMed: 20383134]
8. Monsur Ali M et al. Rolling circle amplification: a versatile tool for chemical biology, materials science and medicine. *Chem. Soc. Rev.* 43, 3324–3341 (2014). [PubMed: 24643375]
9. Lohman GJS, Zhang Y, Zhelkovsky AM, Cantor EJ & Evans TC Jr. Efficient DNA ligation in DNA-RNA hybrid helices by Chlorella virus DNA ligase. *Nucleic Acids Res.* 42, 1831–1844 (2014). [PubMed: 24203707]
10. Lagunavicius A et al. Novel application of Phi29 DNA polymerase: RNA detection and analysis in vitro and in situ by target RNA-primed RCA. *RNA* 15, 765–771 (2009). [PubMed: 19244362]
11. Dirks RM & Pierce NA Triggered amplification by hybridization chain reaction. *Proc. Natl. Acad. Sci. U. S. A.* 101, 15275–15278 (2004). [PubMed: 15492210]
12. Choi HMT, Beck VA & Pierce NA Next-generation in situ hybridization chain reaction: higher gain, lower cost, greater durability. *ACS Nano* 8, 4284–4294 (2014). [PubMed: 24712299]
13. Shah S et al. Single-molecule RNA detection at depth via hybridization chain reaction and tissue hydrogel embedding and clearing. *Development* dev.138560 (2016).
14. Lau JY et al. Significance of serum hepatitis C virus RNA levels in chronic hepatitis C. *Lancet* 341, 1501–1504 (1993). [PubMed: 8099380]
15. Kern D et al. An enhanced-sensitivity branched-DNA assay for quantification of human immunodeficiency virus type 1 RNA in plasma. *J. Clin. Microbiol.* 34, 3196–3202 (1996). [PubMed: 8940471]
16. Battich N, Stoeger T & Pelkmans L Image-based transcriptomics in thousands of single human cells at single-molecule resolution. *Nat. Methods* 10, 1127–1133 (2013). [PubMed: 24097269]
17. Shah S et al. Single-molecule RNA detection at depth by hybridization chain reaction and tissue hydrogel embedding and clearing. *Development* 143, 2862–2867 (2016). [PubMed: 27342713]
18. Nilsson M et al. Padlock probes: circularizing oligonucleotides for localized DNA detection. *Science* 265, 2085–2088 (1994). [PubMed: 7522346]
19. Jin J, Vaud S, Zhelkovsky AM, Posfai J & McReynolds LA Sensitive and specific miRNA detection method using SplintR Ligase. *Nucleic Acids Res.* 44, e116 (2016). [PubMed: 27154271]
20. Besanceney-Webler C et al. Increasing the efficacy of bioorthogonal click reactions for bioconjugation: a comparative study. *Angew. Chem. Int. Ed Engl.* 50, 8051–8056 (2011). [PubMed: 21761519]
21. Padovan-Merhar O et al. Single mammalian cells compensate for differences in cellular volume and DNA copy number through independent global transcriptional mechanisms. *Mol. Cell* 58, 339–352 (2015). [PubMed: 25866248]
22. Kerjaschki D, Sharkey DJ & Farquhar MG Identification and characterization of podocalyxin—the major sialoprotein of the renal glomerular epithelial cell. *J. Cell Biol.* 98, 1591–1596 (1984). [PubMed: 6371025]
23. Horrillo A, Porras G, Ayuso MS & González-Manchón C Loss of endothelial barrier integrity in mice with conditional ablation of podocalyxin (Podxl) in endothelial cells. *Eur. J. Cell Biol.* 95, 265–276 (2016). [PubMed: 27289182]
24. Klemm S et al. Transcriptional profiling of cells sorted by RNA abundance. *Nat. Methods* 11, 549–551 (2014). [PubMed: 24681693]
25. Bushkin Y et al. Profiling T cell activation using single-molecule fluorescence in situ hybridization and flow cytometry. *J. Immunol.* 194, 836–841 (2015). [PubMed: 25505292]

26. Chen F, Tillberg PW & Boyden ES Optical imaging. Expansion microscopy. *Science* 347, 543–548 (2015). [PubMed: 25592419]
27. Chen F et al. Nanoscale imaging of RNA with expansion microscopy. *Nat. Methods* 13, 679–684 (2016). [PubMed: 27376770]
28. Pelliccia F, Gaddini L, Limongi MZ & Rocchi A Visualizing human 5S rDNA. *Chromosome Res.* 5, 205–207 (1997). [PubMed: 9246416]

Online Methods References:

29. Mellis IA, Gupte R, Raj A & Rouhanifard SH Visualizing adenosine-to-inosine RNA editing in single mammalian cells. *Nat. Methods* (2017). doi:10.1038/nmeth.4332

**Figure 1.**

Design and validation of clampFISH technology. **(a)** Schematic of clampFISH probe binding and ligation using CuAAC. **(b)** ClampFISH workflow for doubling fluorescent signal at every round of hybridization. **(c)** Colocalization of GFP mRNA single molecule RNA FISH (left) with GFP mRNA clampFISH round 2 (right; scale bar = 5 μ m) **(d)** Timing and order of clampFISH amplification steps. **(e)** GFP mRNA clampFISH signal on WM983b-GFP cells across 12 rounds of amplification in the presence of click ligation (top) compared to GFP mRNA clampFISH signal in the absence of click ligation (middle). Single cell tracking of

the same cell line without GFP mRNA expression across rounds (below; scale bar = 10 μm). Images are representative single-cells selected from 3-independent experiments. **(f)** mRNA counts per cells across 12 rounds of amplification. **(g)** $\text{Log}_2(\text{intensity})$ of click vs. no click samples across 12 rounds of amplification. **(h)** Density of the $\text{log}_2(\text{intensity})$ of all spots detected at round 12 in click vs. no click samples. **(i)** Mean fluorescence intensity of GFP mRNA clampFISH signal per cell on WM983b-GFP cells across 12 rounds of clampFISH. All graphs are representative of 3-independent experiments.

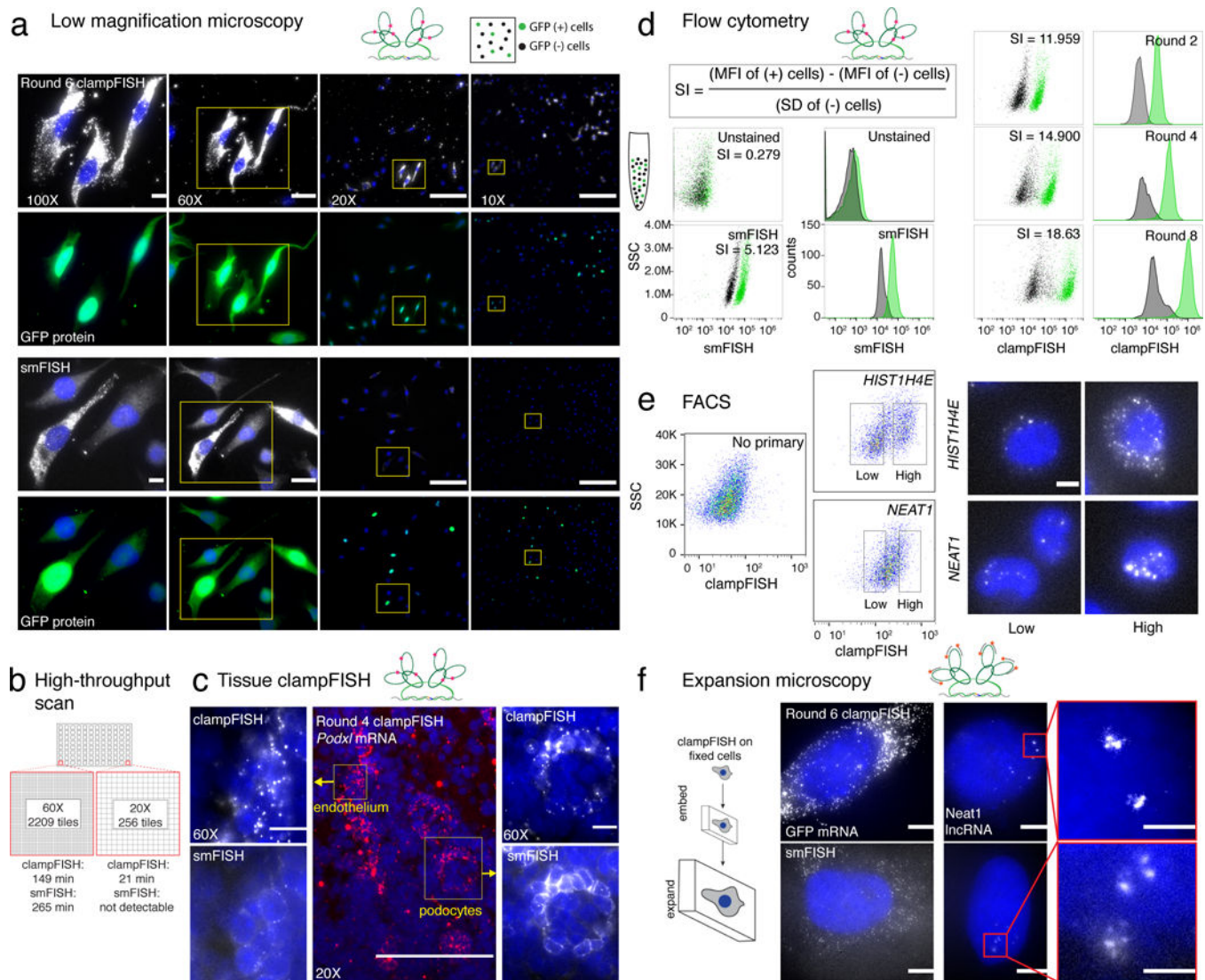


Figure 2. Applications of clampFISH amplification of RNA. **(a)** ClampFISH applied to detect GFP mRNA in a mixed population of WM983b cells and WM983b cells stably expressing GFP (top) and compared to GFP smFISH (bottom) using 0.3 NA 10X, 0.5 NA 20X, 1.4 NA 60X and 1.4 NA 100X magnification objectives (representative images of 2-independent experiments; each image is contrasted independently; scale bars are 10 μ m for 100X and 60X images, 5 μ m for 20X images and 2.5 μ m for 10X images). Each image has a corresponding image showing *GFP* mRNA signal colocalizing with GFP protein. **(b)** Speed of image acquisition for a scan of an individual well from a 96-well plate equivalent. clampFISH at round 6 was compared to that of smFISH at 20X and 60X magnifications. **(c)** (center) 20X image of fixed-frozen 5 μ m 4do mouse kidney section stained with round 4 clampFISH probes targeting *Podxl*. (left) 60X image of mouth endothelium by round 4 clampFISH and by single molecule RNA FISH. (right) 60X image of podocyte by round 4 clampFISH and by single molecule RNA FISH (representative images shown of 2-independent experiments). **(d)** clampFISH was applied to a mixed population of MDA-MB

231 cells with and without GFP expression and analyzed by flow cytometry across 8 rounds of amplification. Cells were gated on *GFP* expression and are displayed in green. (e) *HIST1H4E* mRNA and *NEAT1* lncRNA were amplified to 6 rounds with clampFISH probes on HeLa cells and cells were separated using a flow sorter. High and low expressers were collected and imaged by microscopy (scale bar is 20 μm). (f) (top) Fluorescent micrographs of round 6 clampFISH targeting *GFP* mRNA and Neat1 lncRNA in cultured WM983b-GFP cells (bottom) fluorescent micrographs of single molecule RNA FISH targeting *GFP* mRNA and *NEAT1* lncRNA in cultured WM983b-GFP cells using the same dye (images representative of 2-independent experiments; scale bars are 20 μm for the images, and 5 μm for the inlay).

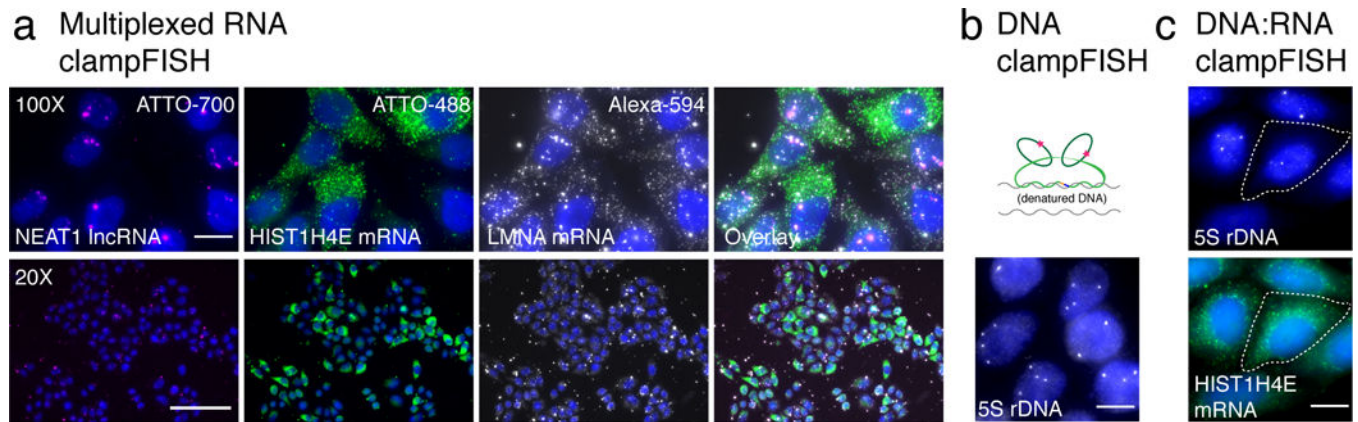


Figure 3. Multiplexing of amplified RNA and DNA targets. **(a)** Fluorescent micrographs of individual probe channels: (from left) *NEAT1* lncRNA labeled with ATTO700, *HIST1H4E* mRNA labeled with ATTO 488, and *LMNA* mRNA labeled with Alexa 594 and an overlay on the far right. (top) 100X magnification with 20 μm scale bars, (bottom) 20X magnification with 20 μm scale bars. Images are representative of 2 independent experiments. **(b)** DNA clampFISH of 5S rDNA was performed to 2 rounds on HeLa cells and detected in Cy5. **(c)** Multiplexed DNA and RNA clampFISH of *HIST1H4E* and DNA clampFISH of 5S rDNA on HeLa cells.